Mon. Not. R. Astron. Soc. **379,** 605–618 (2007) doi:10.1111/j.1365-2966.2007.11864.x

The differentially rotating force-free magnetosphere of an aligned rotator: analytical solutions in the split-monopole approximation

A. N. Timokhin[1,2]★

[1]*Physics Department, Ben-Gurion University of the Negev, POB 653, 84105 Beer-Sheva, Israel*
[2]*Sternberg Astronomical Institute, Universitetskij pr. 13, 119992 Mocsow, Russia*

Accepted 2007 April 16. Received 2007 February 27

ABSTRACT

In this paper we consider the stationary force-free magnetosphere of an aligned rotator when the plasma in the open field-line region rotates differentially as a result of the presence of a zone with an accelerating electric field in the polar cap of the pulsar. We study the impact of differential rotation on the current density distribution in the magnetosphere. Using the split-monopole approximation we obtain analytical expressions for the physical parameters of the differentially rotating magnetosphere. We find the range of admitted current density distributions under the requirement that the potential drop in the polar cap is less than the vacuum potential drop. We show that the current density distribution could deviate significantly from the 'classical' Michel distribution and could be made almost constant over the polar cap, even when the potential drop in the accelerating zone is of the order of 10 per cent of the vacuum potential drop. We argue that the differential rotation of the open magnetic field lines could play an important role in adjusting the current density between the magnetosphere and the polar-cap cascade zone and could affect the value of the pulsar braking index.

Key words: MHD – stars: neutron – pulsars: general.

1 INTRODUCTION

The physics of radiopulsars is still not fully understood, despite the substantial efforts of many theoreticians in the field. It is generally assumed that a radiopulsar has an MHD-like magnetosphere that is very close to being force-free, except in some geometrically small regions – the model first introduced by Goldreich & Julian (1969). For many years the solution of force-free MHD equations was a problem, even for the simplest case of an aligned pulsar. Now, however, it is possible to solve the Grad–Shafranov equation describing the structure of a force-free magnetosphere of an aligned pulsar (see e.g. Contopoulos, Kazanas & Fendt 1999; Goodwin et al. 2004; Gruzinov 2005; Timokhin 2006). Stationary magnetosphere configurations for an aligned rotator were also obtained as the final stage in non-stationary numerical modelling (Komissarov 2006; McKinney 2006; Bucciantini et al. 2006; Spitkovsky 2006). Even the case of an inclined rotator has been studied numerically (Spitkovsky 2006). The pulsar magnetosphere is a very complicated physical system, however, because most of the current carriers (electrons and positrons) are produced inside the system, in the polar-cap cascades. The production of electron–positron pairs is a process with a threshold, so it can operate only under specific conditions, and, generally speaking, not every current density can flow through the cascade zone.

★E-mail: atim@sai.msu.ru

In magnetohydrodynamics (MHD), the current density distribution is not a free 'parameter'; it is obtained in the course of solving the MHD equations. In the case of pulsars, however, obtaining a solution for the MHD equations does not solve the problem, because it is possible that the polar-cap cascade zone will not be able to provide the required current density distribution, and, hence, will be unable to support the configuration of the magnetosphere corresponding to the solution of the MHD equations. In terms of MHD, the polar-cap cascade zone sets complicated boundary conditions at the foot points of the open magnetic field lines, and any self-consistent solution of the problem must match them. The most 'natural' configuration of the magnetosphere of an aligned rotator, in which the last closed field line extends up to the light cylinder, requires a current density distribution that could not be supported by stationary electromagnetic cascades in the polar cap of the pulsar (see Timokhin 2006, hereafter Paper I). This configuration requires that in some parts of the polar cap the electric current flows against the preferred direction of the accelerating electric field. This configuration also seems to be impossible for non-stationary cascades, although this problem requires further careful investigation (Fawley 1978; Al'Ber, Krotova & Eidman 1975; Levinson et al. 2005). The structure of the magnetosphere should thus be different from this simple picture. The magnetosphere of a pulsar should have a configuration with a current density distribution that can flow through the polar-cap cascade zone without the suppression of electron–positron pair creation. Whether such a configuration exists is an open question; in

other words, the possibility that the real pulsar magnetosphere has large domains where the MHD approximation is broken cannot be completely excluded (see e.g. Arons 1979; Michel 1991).

As the pulsar magnetosphere and the polar-cap cascade zone have very different characteristic time-scales, it is virtually impossible to model the whole system at once. These physical systems should therefore be modelled separately, and the whole set of solutions for each system should be found in order to find compatible ones. We thus suggest the following approach to the construction of the pulsar magnetosphere model: determine which currents could flow through the force-free pulsar magnetosphere, and then compare them with the currents able to flow through the polar-cap cascade zone. In this work we deal with the first part of this suggested 'program': we consider the range of possible current density distributions in the force-free magnetosphere of an aligned rotator.

The force-free magnetosphere of an aligned rotator is the simplest possible case of an MHD-like pulsar magnetosphere and needs to be the first to be investigated. This system has two physical degrees of freedom: (i) the size of the closed field line zone, and (ii) the distribution of the angular velocity of the open magnetic field lines. In each stationary configuration the current density distribution is fixed. Considering different configurations by changing (i) and (ii) and keeping them in a reasonable range, the whole set of admitted current density distributions can be found. The differential rotation of the open field lines is caused by variation of the accelerating electric potential in the cascade zone across the polar cap. Theories of stationary polar-cap cascades predict a small potential drop, and in this case only one degree of freedom is left – the size of the zone with closed magnetic field lines. This case was studied in detail in Paper I, with the finding that stationary polar-cap cascades are incompatible with a stationary force-free magnetosphere. The polar-cap cascades therefore probably operate in the non-stationary regime. For non-stationary cascades the average potential drop in the accelerating zone could be larger than the drop maintained by stationary cascades. Hence, the open magnetic field lines may rotate with significantly different angular velocities even in the magnetospheres of young pulsars. On the other hand, for old pulsars the potential drop in the cascade zone is large, and the magnetospheres of such pulsars should rotate essentially differentially.

The case of a differentially rotating pulsar magnetosphere has not been investigated in detail before, although some authors have addressed the case in which the open magnetic field lines rotate with a constant angular velocity different from that of the neutron star (NS), see e.g. Beskin, Gurevich & Istomin (1993) and Contopoulos (2005). The first attempt to construct a self-consistent model of a pulsar magnetosphere with a *differentially* rotating open field line zone was made in Timokhin 2007, hereafter Paper II. In that paper we considered only the case for which the angular velocity of the open field lines is lower than the angular velocity of the NS. We have shown that the current density can be made almost constant over the polar cap, although at a cost of a large potential drop in the accelerating zone. The angular velocity distributions was chosen on an ad hoc basis, and an analysis of the admitted range for current density distributions was not performed.

In this paper we discuss the properties of the differentially rotating magnetosphere of an aligned rotator in general, and elaborate the limits on the differential rotation. We study in detail the case in which the current density in the polar cap is a linear function of the magnetic flux. It allows us to obtain the main relationships analytically. We find the range within which the physical parameters of the magnetosphere could vary, requiring that (i) the potential drop in the polar cap is not greater than the vacuum potential drop, and (ii) the current in the polar cap does not change its direction.

The plan of the paper is as follows. In Section 2 we discuss the basic properties of the differentially rotating force-free magnetosphere of an aligned rotator and derive equations for the angular velocity distribution, the current density, and the Goldreich–Julian charge density in the magnetosphere. In Section 3 we derive equations for the potential drop that supports configurations with a linear current density distribution in the polar cap of the pulsar and give their general solutions. In Section 4 we analyse the physical properties of admitted magnetosphere configurations: the current density distribution, the maximum potential drop, the angular velocity of the open magnetic field lines, the Goldreich–Julian current density, the spindown rate and the total energy of the magnetosphere. At the end of that section we consider as examples two sets of solutions, one with constant current densities and the other with the smallest potential drops. In Section 5 we summarize the results, discuss the limitations of the used approximation, and briefly describe possible modifications of the obtained solutions that will arise in truly self-consistent models. In that section we also discuss how the differential rotation affects the value of the pulsar braking index.

2 DIFFERENTIALLY ROTATING MAGNETOSPHERE: BASIC PROPERTIES

2.1 Pulsar equation

Here, as in Papers I and II, we consider the magnetosphere of an aligned rotator that is at the coordinate origin and has a dipolar magnetic field. We use normalizations similar[1] to the ones in Paper I, but now we write all equations in the spherical coordinates (r, θ, ϕ). We normalize all distances to the light-cylinder radius of the corotating magnetosphere $R_{\rm LC} \equiv c/\Omega$, where Ω is the angular velocity of the NS, and c is the speed of light. For the axisymmetric case considered, the magnetic field can be expressed through the two dimensionless scalar functions Ψ and S as (cf. equation 8 in Paper I)

$$\boldsymbol{B} = \frac{\mu}{R_{\rm LC}^3} \frac{\nabla\Psi \times \boldsymbol{e}_\phi + S\boldsymbol{e}_\phi}{r\sin\theta}, \tag{1}$$

where $\boldsymbol{e}_\phi$ is the unit azimuthal, toroidal vector; $\mu = B_0 R_{\rm NS}^3/2$ is the magnetic moment of the NS; B_0 is the magnetic field strength at the magnetic pole; and $R_{\rm NS}$ is the radius of the NS. The scalar function Ψ is related to the magnetic flux as $\Phi_{\rm mag}(\varpi, Z) = 2\pi(\mu/R_{\rm LC})\,\Psi(r, \theta)$. $\Phi_{\rm mag}$ is the magnetic flux through a circle of radius $\varpi = r\sin\theta$ with its centre at the point on the rotation axis at a distance $Z = r\cos\theta$ from the NS. The lines of constant Ψ coincide with the magnetic field lines. The scalar function S is related to the total current J *outflowing* through the same circle by the equation $J(\varpi, Z) = 1/2(\mu/R_{\rm LC}^2)\,c\,S(r, \theta)$.

The electric field in the force-free magnetosphere is given by

$$\boldsymbol{E} = -\frac{\mu}{R_{\rm LC}^3}\,\beta\,\nabla\Psi, \tag{2}$$

where β is the ratio of the angular velocity of the rotation of the magnetic field lines, $\Omega_{\rm F}$, to the angular velocity of the NS: $\beta \equiv \Omega_{\rm F}/\Omega$ (cf. equation 14 in Paper I). The difference between the angular velocity of a magnetic field line and the angular velocity of the NS is caused by a potential drop along the field line in the polar-cap acceleration zone.

[1] Note that here, in contrast to in Paper I, Ψ is already dimensionless.

For these dimensionless functions the equation describing the stationary force-free magnetosphere, the so-called pulsar equation (Michel 1973a; Scharlemann & Wagoner 1973; Okamoto 1974), takes the form (cf. equation 20 in Paper I)

$$[1-(\beta r\sin\theta)^2]\Delta\Psi - \frac{2}{r}\left(\partial_r\Psi + \frac{\cos\theta}{\sin\theta}\frac{\partial_\theta\Psi}{r}\right) + S\frac{\mathrm{d}S}{\mathrm{d}\Psi} - \beta\frac{\mathrm{d}\beta}{\mathrm{d}\Psi}(r\sin\theta\,\nabla\Psi)^2 = 0. \quad (3)$$

This equation express the force balance across the magnetic field lines. At the light cylinder $1-(\beta r\sin\theta)^2$ goes to zero and the pulsar equation reduces to

$$S\frac{\mathrm{d}S}{\mathrm{d}\Psi} = \frac{1}{\beta}\frac{\mathrm{d}\beta}{\mathrm{d}\Psi}(\nabla\Psi)^2 + 2\beta\sin\theta\,(\partial_r\Psi + \beta\cos\theta\,\partial_\theta\Psi). \quad (4)$$

Each smooth solution must satisfy these two equations, and the problem of solving the pulsar equations transforms to an eigenfunction problem for the poloidal current function S (see, for example, section 2.3 in Paper I). Equation (4) could also be considered as an equation for the poloidal current.

We adopt for the magnetosphere the configuration with the so-called Y-null point. That is, we assume that the magnetosphere is divided into two zones, the first one with closed magnetic field lines, which extend from the NS up to the neutral point, located at a distance x_0 from the NS, and the second one with magnetic field lines that are open and extend to infinity (see Fig. 1). In the closed magnetic field line zone, plasma corotates with the NS, there is no poloidal current along field lines, and the magnetic field lines

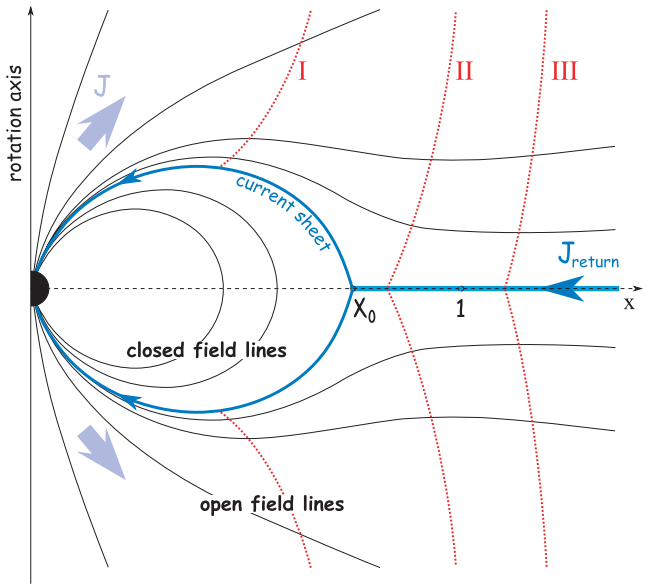

Figure 1. Structure of the magnetosphere of an aligned rotator (schematic picture). Magnetic field lines are shown by solid lines. The outflowing current J along open magnetic field lines and the returning current $J_{\rm return}$ in the current sheet, separating zones of open and closed magnetic field lines, are indicated by arrows. The current sheet is along the last open magnetic field line, corresponding to the value of the flux function $\Psi_{\rm pc}$. Distances are measured in units of the light-cylinder radius for the corotating magnetosphere $R_{\rm LC}$, i.e. the point at $x=1$ marks the position of the light cylinder in the corotating magnetosphere. The null point x_0 could lie anywhere inside the interval [0, 1]. Possible positions of the real light cylinder are shown by dotted lines. Line I corresponds to the case with $1/\beta(\Psi_{\rm pc}) < x_0$; line II, to $x_0 < 1/\beta(\Psi_{\rm pc}) < 1$; and line III, to $1 < 1/\beta(\Psi_{\rm pc})$ (see text for further details).

there are equipotential. Obviously this zone cannot extend beyond the light cylinder. In the rest of the magnetosphere, magnetic field lines are open owing to the poloidal current produced by outflowing charged particles. The return current, needed to keep the NS charge neutral, flows in a thin region (current sheet) along the equatorial plane and then along the last open magnetic field line. We assume that this picture is stationary on the time-scale of the order of the period of rotation of the NS. As was outlined in Paper I, the polar-cap cascades in pulsars are probably non-stationary. The characteristic time-scale of the polar-cap cascades, $\sim h/c \sim 3\times10^{-5}$ s (where h is the length of the acceleration zone, being of the order of $R_{\rm NS}$), is much shorter that the pulsar period (which for most pulsars is $\gg10^{-3}$ s). So, for the global magnetosphere structure only the time averages of the physical parameters connected to the cascade zone are important. In the rest of the paper, when we discuss physical parameters set by the cascade zone we will always mean the *average* values of them, unless explicitly stated otherwise.

The differential rotation of the open magnetic field lines that is caused by the presence of a zone with an accelerating electric field in the polar cap of a pulsar (i) contributes to the force balance across the magnetic field lines (the last term in equation 3), (ii) modifies the current density in the magnetosphere (the first term on the right-hand side of equation 4), and (iii) changes the position of the light cylinder, where condition (4) must be satisfied. Note that for (i) and (ii) the derivative $\mathrm{d}\beta/\mathrm{d}\Psi$, i.e. the form of the distribution $\beta(\Psi)$, plays an important role. Therefore for different angular velocity distributions in the open magnetic field line zone there should exist different magnetosphere configurations that have in general distinct current density distributions. Let us now consider restrictions on the differential rotation rate $\beta(\Psi)$.

2.2 Angular velocity of the open magnetic field lines

As a result of the rotation of the NS a large potential difference arises between the magnetic field-line foot points on the surface of the NS. The potential difference between the pole and the magnetic field line corresponding to the value of the magnetic flux function Ψ is

$$\Delta\mathcal{V}(\Psi) = \frac{\mu}{R_{\rm LC}^2}\Psi. \quad (5)$$

In a perfectly force-free magnetosphere the magnetic field lines are equipotential. Owing to the presence of the polar-cap acceleration zone, where MHD conditions are not satisfied, however, part of this potential difference appears as a potential drop between the surface of the NS and the pair-formation front, above which the magnetic field line remains equipotential. This potential drop is the reason why the open magnetic field lines rotate differently from the NS. The normalized angular velocity of a magnetic field line β is expressed through the potential drop along the field line as (e.g. Beskin 2005, Paper I)

$$\beta = 1 + \frac{R_{\rm LC}^2}{\mu}\frac{\partial V(\Psi)}{\partial\Psi}. \quad (6)$$

$\mathcal{V}$ is the total potential drop (in statvolts) along the magnetic field line in the polar-cap acceleration zone (cf. equation 23 in Paper I).

The polar cap of a pulsar is limited by the magnetic field line corresponding to a value of the flux function $\Psi_{\rm pc}$. The potential drop between the rotation axis and the boundary of the polar cap is

$$\Delta\mathcal{V}(\Psi_{\rm pc}) = \frac{\mu}{R_{\rm LC}^2}\Psi_{\rm pc} \equiv \Delta\mathcal{V}_{\rm pc}. \quad (7)$$

This is the maximum available potential drop along an open magnetic field line. It could be achieved in a vacuum, when there is no

plasma in the polar cap. We will call $\Delta\mathcal{V}_{\rm pc}$ the vacuum potential drop. Let us normalize the poloidal flux function Ψ to its value at the last open magnetic field line $\Psi_{\rm pc}$ and introduce a new function $\psi \equiv \Psi/\Psi_{\rm pc}$. Normalizing the potential drop along field lines to the vacuum potential drop and introducing the dimensionless function $V \equiv \mathcal{V}/\Delta\mathcal{V}_{\rm pc}$, we rewrite the expression for the normalized angular velocity of the open magnetic field line as

$$\beta = 1 + \frac{\partial V}{\partial \psi}. \tag{8}$$

As the potential drop *along* any field line cannot be greater than the vacuum drop and cannot have a different sign from the vacuum drop, the variation of the electric potential *across* the polar cap cannot exceed the vacuum potential drop. In terms of the dimensionless functions this condition has the form

$$|V(\psi_1) - V(\psi_2)| \leqslant 1, \quad \forall\, \psi_1, \psi_2 \in [0, 1]. \tag{9}$$

The inequality (9) sets the limit on the electric potential in the polar cap of a pulsar.

2.3 Current density in the polar cap

In order to obtain the current density distribution in the polar cap of a pulsar, the pulsar equation (3) together with the condition at the light cylinder (4) must be solved. There is an analytical solution of the pulsar equation only for a split-monopole configuration of the poloidal magnetic field. That is, when the flux function Ψ has the form

$$\Psi = \Psi_{\rm M}(1 - \cos\theta), \tag{10}$$

$\Psi_{\rm M}$ being a constant, equations (3) and (4) have a smooth solution if the poloidal current function S has the form (e.g. Blandford & Znajek 1977)

$$S(\Psi) = -\beta(\Psi)\,\Psi\left(2 - \frac{\Psi}{\Psi_{\rm M}}\right). \tag{11}$$

Here $\Psi_{\rm M}$ corresponds to the value of the magnetic flux through the upper hemisphere, i.e. it corresponds to the magnetic field line lying in the equatorial plane. The poloidal current given by equation (11) is very similar to the current in the well-known Michel solution (Michel 1973b), but this expression is valid for non-constant $\beta(\Psi)$ too.

In this paper we will use expression (11) for the poloidal current function S. In doing so, we assume that in the neighbourhood of the light cylinder the geometry of the poloidal magnetic field is close to a split monopole. This is a good approximation if the size of the closed magnetic field-line zone is much smaller than the light-cylinder size, i.e. $x_0 \ll 1/\beta(\psi)$, $\psi < 1$. For configurations in which the edge of the corotating zone[2] approaches the light cylinder, the poloidal current S is different from that given by equation (11), but we expect that this deviation should not exceed 10–20 per cent. Indeed, in the numerical simulations described in Paper I, where the case of constant $\beta \equiv 1$ was considered, the deviation of S from Michel's poloidal current did not exceed 20 per cent and it became smaller for smaller sizes of the corotating zone (see fig. 3 in Paper I). Similarly, in Paper II, in which we considered the case of variable $\beta < 1$, the poloidal current deviated from the values given by the analytical formula (11) by less than 20 per cent and the difference became smaller for smaller sizes of the corotating zone. We may therefore hope that the same relationship holds in the general case too.

We intend to find the range of admitted current density distributions in the force-free magnetosphere. Here we use the split-monopole approximation for the poloidal current (11), and hence we can study the effect of only the differential rotation on the current density distribution. The dependence of the current density on the size of the corotating zone in a differentially rotating magnetosphere will be addressed in a subsequent paper, in which we will refine our results by performing numerical simulations for different sizes of the corotating zone.

Thus in our approximation the last closed field line in the dipole geometry corresponds to the field line lying in the equatorial plane in the monopole geometry, i.e. $\Psi_{\rm M} = \Psi_{\rm pc}$. In normalized variables, the expression for the poloidal current has the form

$$S(\Psi) = -\Psi_{\rm pc}\,\beta(\psi)\,\psi(2 - \psi). \tag{12}$$

The poloidal current density in the magnetosphere is (see e.g. Beskin 2005)

$$j_{\rm pol} = \frac{c}{4\pi}\frac{\mu}{R_{\rm LC}^4}\frac{\nabla S \times \boldsymbol{e}_\phi}{r\sin\theta} = \frac{\Omega \boldsymbol{B}_{\rm pol}}{2\pi c}c\,\frac{1}{2}\frac{{\rm d}S}{{\rm d}\Psi}. \tag{13}$$

In the polar cap of the pulsar the magnetic field is dipolar and, hence, poloidal. The Goldreich–Julian charge density for the corotating magnetosphere near the NS is

$$\rho^0_{\rm GJ} = -\frac{\boldsymbol{\Omega}\cdot\boldsymbol{B}}{2\pi c}. \tag{14}$$

Using expressions (12)–(14) we obtain for the current density in the polar cap of the pulsar

$$j = \frac{1}{2}j^0_{\rm GJ}\left[2\beta(1-\psi) + \beta'\psi(2-\psi)\right]. \tag{15}$$

The prime denotes differentiation with respect to ψ, i.e. $\beta' \equiv {\rm d}\beta/{\rm d}\psi$; and $j^0_{\rm GJ} \equiv \rho^0_{\rm GJ}\,c$ is the Goldreich–Julian current density in the polar cap for the *corotating* magnetosphere. At the surface of the NS, where the potential drop is zero and the plasma corotates with the NS, $j^0_{\rm GJ}$ corresponds to the local GJ current density.

2.4 Goldreich–Julian charge density in the polar cap for a differentially rotating magnetosphere

The Goldreich–Julian (GJ) charge density is the charge density that supports the force-free electric field:

$$\rho_{\rm GJ} \equiv \frac{1}{4\pi}\nabla\cdot\boldsymbol{E}. \tag{16}$$

The GJ charge density at points along a magnetic field line rotating with an angular velocity different from the angular velocity of the NS will be different from the values given by equation (14). Substituting the expression for the force-free electric field (2) into equation (16) we obtain

$$\rho_{\rm GJ} = -\frac{\mu}{4\pi R_{\rm LC}^4}\left(\beta\Delta\Psi + \beta'(\nabla\Psi)^2\right). \tag{17}$$

We see that the GJ charge density depends not only on the angular velocity of the field-line rotation (the first term in equation 17), but also on the angular velocity profile (the second term in equation 17).

Near the NS the magnetic field is essentially dipolar. The magnetic flux function Ψ for a dipolar magnetic field is

$$\Psi^{\rm dip} = \frac{\sin^2\theta}{r}. \tag{18}$$

[2]Plasma in the closed field-line zone corotates with the NS, so we will call the region with the closed magnetic field lines the corotating zone.

Substituting this expression into equation (17) we obtain

$$\rho_{\rm GJ} = -\frac{\mu}{4\pi R_{\rm LC}^4}\,\frac{1}{r^3} \times \left(\beta\, 2(3\cos^2\theta - 1) + \beta'\frac{\sin^2\theta}{r}(3\cos^2\theta + 1)\right). \quad (19)$$

In the polar cap of the pulsar $\cos\theta \simeq 1$ and $\mu/(rR_{\rm LC})^3 \simeq B/2$. Recalling the expression for the magnetic flux function for a dipolar magnetic field (18), we obtain for the local GJ charge density in the polar cap of the pulsar the expression

$$\rho_{\rm GJ} = \rho^0_{\rm GJ}\,(\beta + \beta'\psi). \quad (20)$$

3 ACCELERATING POTENTIAL

In our approximation, any current density distribution in the force-free magnetosphere of an aligned rotator has the form given by equation (15). The current density depends on the angular velocity of the magnetic field lines $\beta(\psi)$, which for a given field line depends on the total potential drop along that line according to equation (8). The potential drop in the acceleration zone cannot exceed the vacuum potential drop, i.e. V is limited by inequality (9).

Therefore, if we wish to find the accelerating potential that supports a force-free configuration of the magnetosphere for a given form of the current density distribution[3] in the polar cap we do the following. We equate the expression for the current density distribution to the general expression for the current density (15), and then express $\beta(\psi)$ in terms of $V(\psi)$ by means of equation (8), thus obtaining an equation for the electric potential V that supports a force-free magnetosphere configuration with the desired current density distribution. If solutions of the obtained equation fulfil limitation (9), such a configuration is admitted; if not, such a current density could not flow in the force-free magnetosphere of an aligned pulsar. At present there is no detailed model for non-stationary polar-cap cascades from which we could deduce reasonable shapes for the current density distribution. We therefore try to set constrains on the current density by assuming the linear dependence of the current density on ψ.

In a differentially rotating magnetosphere there are two characteristic current densities. The first one is the Goldreich–Julian current density for the corotating magnetosphere, $j^0_{\rm GJ}$. It corresponds to the actual Goldreich–Julian current density in the magnetosphere at the NS surface, where differential rotation has not yet been built up. The second characteristic current density is the actual Goldreich–Julian current density, $j_{\rm GJ}$, at points above the acceleration zone, where the magnetosphere is already force-free and the final form of the differential rotation is established; in the polar cap $j_{\rm GJ}$ is given by formula (20). For a magnetosphere with a strong differential rotation, the current densities $j^0_{\rm GJ}$ and $j_{\rm GJ}$ differ significantly. In this section we consider both cases; that is, when the current density distribution is normalized to $j^0_{\rm GJ}$ and when it is normalized to $j_{\rm GJ}$.

3.1 Outflow with the current density being a constant fraction of the actual Goldreich–Julian current density

For non-stationary cascades the physics is determined by the response of the cascade zone to the inflowing particles and MHD waves coming from the magnetosphere. However, the accelerating electric field depends on the deviation of the charge density from the local value of the GJ charge density. Thus the first naive guess would be that the preferred state of the cascade zone would be the state in which (on average) the current density is equal to the GJ current density $j_{\rm GJ}$:

$$j(\psi) = j_{\rm GJ}(\psi) = j^0_{\rm GJ}\,(\beta + \beta'\psi). \quad (21)$$

Equating this formula to the general expression for the current density (15) and substituting for β with expression (8), we obtain after algebraical manipulation the equation for the accelerating electric potential in the polar cap of the pulsar:

$$V'' = -2\,\frac{1 + V'}{\psi}. \quad (22)$$

We set the boundary conditions for V at the edge of the polar cap. As the boundary conditions we can use the value of the normalized angular velocity at the edge of the polar cap and the value of the electric potential there:

$$1 + V'(1) = \beta_{\rm pc}, \quad (23)$$

$$V(1) = V_0. \quad (24)$$

The solution of equation (22) satisfying the boundary conditions (24), (23) is

$$V(\psi) = V_0 + (1 - \psi)\left(1 - \frac{\beta_{\rm pc}}{\psi}\right). \quad (25)$$

We see that, unless $\beta_{\rm pc} = 0$, the potential has a singularity on the rotation axis, and, hence, such a configuration cannot be realized in the force-free magnetosphere of a pulsar. Condition (9) is violated – the potential difference exceeds the vacuum potential drop.

If $\beta_{\rm pc} = 0$, the potential is $V = V_0 + 1 - \psi$, and from equation (8) we have $\beta(\psi) \equiv 0$. Substituting this into equation (15) we obtain for the current density $j(\psi) \equiv 0$. Thus the case with $\beta_{\rm pc} = 0$ is degenerate: as there is no poloidal current in the magnetosphere, it corresponds to the vacuum solution.

Let us now consider a more general form for the current density distribution:

$$j(\psi) = A\,j_{\rm GJ}(\psi) = A\,j^0_{\rm GJ}\,(\beta + \beta'\psi), \quad (26)$$

where A is a constant. In this case for the accelerating electric potential in the polar cap of the pulsar we have the equation

$$V'' = 2(1 + V')\frac{1 - A - \psi}{\psi\,[\psi + 2(A - 1)]}. \quad (27)$$

For the same boundary conditions (24), (23), the solution of this equation is

$$V(\psi) = V_0 + 1 - \psi + \frac{\beta_{\rm pc}(2A - 1)}{2(A - 1)}\log\left[\frac{\psi(2A - 1)}{\psi + 2(A - 1)}\right]. \quad (28)$$

This solution is valid for $A \neq 1,\ 1/2$. There is the same problem as above with the electric potential in this solution. Namely, unless $\beta_{\rm pc} = 0$ the potential V is singular[4] on the rotation axis. The case with $A = 1/2$ is also degenerate, because in that case the solution for the electric potential is $V(\psi) = V_0 + 1 - \psi$, which yields the current density $j(\psi) \equiv 0$.

We see that solutions in which the current density is a constant fraction of the actual GJ current density are not allowed, except for a trivial degenerate case, corresponding to no net particle flow.

[3]Guessed from a model for the polar-cap cascades, for example.

[4]The singularity arises because $V''(0)$ goes to infinity unless $1 + V'(0) = \beta(0)$ is zero, as follows from equation (27).

The naive physical picture does not work, and the current density in the magnetosphere in terms of the actual GJ current density must vary across the polar cap. On the other hand, the GJ current density is itself a variable function across the polar cap; it also changes with altitude within the acceleration zone, where the potential drop increases until it reaches its final value. We therefore find it more convenient to consider the current density in terms of the corotational GJ current density.

3.2 Outflow with the current density as a linear function of the magnetic flux in terms of the corotational Goldreich–Julian current density

In models with space charge-limited flow (SCLF), in which charged particles can freely escape from the NS surface (e.g. Scharlemann, Arons & Fawley 1978), the charge density at the NS surface is always equal to the local GJ charge density there, i.e. $(\rho = \rho^0_{\rm GJ})|_{r=R_{\rm NS}}$. For SCLF, the actual current density in the polar cap could be less than $j^0_{\rm GJ}$ if the acceleration of the particles is periodically blocked in the non-stationary cascades. The current density could be greater than $j^0_{\rm GJ}$ if there is an inflow of particles having an opposite charge to that of the GJ charge density from the magnetosphere into the cascade zone (e.g. Lyubarskij 1992). Therefore, an expression for the current density in terms of the corotational GJ current density $j^0_{\rm GJ}$ would be more informative from the point of view of the cascade physics than an expression in terms of the local GJ current density $\boldsymbol{j}_{\rm GJ}$.

Let us consider the case in which the current density distribution in the polar cap of the pulsar has the form

$$j = j^0_{\rm GJ}(a\psi + b), \tag{29}$$

where a, b are constants. The Michel current density distribution is a particular case of this formula and corresponds to the values $a = -1$, $b = 1$. The equation for the electric potential for this current density is

$$V'' = 2\,\frac{a\psi + b - (1+V')(1-\psi)}{\psi(2-\psi)}. \tag{30}$$

The solution of equation (30) satisfying the boundary conditions (24), (23) is

$$V(\psi) = V0 + (1+a)(1-\psi) + \frac{1}{2}\log[(2-\psi)^{-\beta_{\rm pc}-3a-2b}\psi^{\beta_{\rm pc}-a-2b}]. \tag{31}$$

We see that the potential is non-singular on the rotation axis if $\beta_{\rm pc} = a + 2b$. The admitted solution for the electric potential is therefore

$$V(\psi) = V0 + (1+a)(1-\psi) - 2(a+b)\log(2-\psi). \tag{32}$$

In the rest of the paper we will use expression (32) for the electric potential. We will analyse the physical properties of force-free magnetosphere configurations when the electric potential in the acceleration zone of the polar cap has this form.

4 PROPERTIES OF ADMITTED CONFIGURATIONS

4.1 Admitted current density

The potential drop in the polar cap of the pulsar is limited by the vacuum potential drop. In our notation, this limit is formulated as inequality (9). Parameters a, b from the expression for the electric current (29) enter into the formula for the electric potential (32). Imposing limitation (9) we obtain the admitted range for these parameters in the force-free magnetosphere. In Appendix A we carry out such an analysis and find the region in the plane (a, b) that is admitted by requirement (9). This region is shown as the grey area in Fig. A1. From Fig. A1 it is evident that for most of the admitted values of the parameters a, b the current density has different signs in different parts of the polar cap. There is also a region where the values of the parameters correspond to the current density distributions having the same sign as the GJ charge density in the whole polar cap.

The physics of the polar-cap cascades imposes additional limitations on the current density and accelerating electric potential distribution in the polar cap. There is at present no detailed theory of non-stationary polar-cap cascades. In setting constraints on the current density distribution we should therefore use simple assumptions about the possible current density. There is a preferred direction for the accelerating electric field in the polar cap. The direction of this field is such that it accelerates charged particles having the same sign as the GJ charge density away from the star. It is natural to assume that the average current in the polar-cap cascade should flow in the same direction. The average current could flow in the opposite direction only if the accelerating electric field were screened. In order to screen the accelerating field a sufficient number of particles of the same sign as the accelerated ones should come from the magnetosphere and penetrate the accelerating potential drop. These particles, however, are themselves produced in the polar-cap cascade. They must be reversed somewhere in the magnetosphere and be accelerated up to an energy comparable with the energy the primary particles receive in the polar-cap cascade. Even if the problem of particle acceleration back to the NS could be solved, screening of the electric field will interrupt the particle creation, and, hence, there will not be enough particles in the magnetosphere to screen the electric field at the next moment of time. Although the real physics is more complicated and is not yet fully understood, the case of the unidirectional current in the polar cap is worthy of detailed investigation, as it is 'the most natural' from the point of view of the polar-cap cascade physics. In the following we will call current of the same sign as the GJ charge density 'positive', and current of the opposite sign to the GJ charge density 'negative'.

The linear current density distribution (29) will be always positive if

$$b \geqslant \max(-a, 0). \tag{33}$$

Only a subset of the admitted values of a, b corresponds to a positive current density distribution. Such values of the parameters a, b are inside the triangle-like region shown in Figs 2, 3 and 4. We see that a wide variety of positive current density distributions are admitted in the force-free magnetosphere: current density distributions that are constant across the polar cap of the pulsar are admitted, as are current densities decreasing or increasing towards the polar-cap boundary. The current density in the force-free magnetosphere could therefore deviate strongly from the classical Michel current density, corresponding to the point $a = -1$, $b = 1$. The price for this freedom is the presence of a non-zero accelerating electric potential in the polar cap. If the price for a particular current density distribution is too high, that is, if the potential drop is too large, only the magnetosphere of a very old pulsar could admit such a current density. Let us now consider the distribution of the potential drop in the parameter space (a, b).

4.2 Electric potential

We have already emphasized that the shape of the function $V(\psi)$ is very important for the resulting current density distribution.

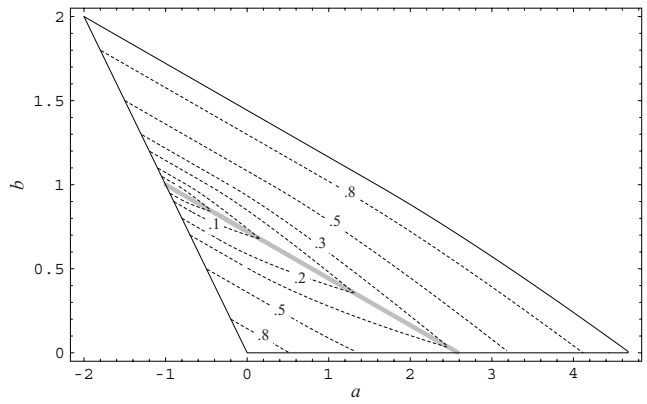

Figure 2. Maximum potential drop across the polar cap. The dotted lines show contours of $\Delta V_{\rm max}$: contours for $\Delta V_{\rm max} = 0.05$, 0.1, 0.2, 0.3, 0.5, 0.8 are shown, with labels corresponding to the values of $\Delta V_{\rm max}$. The line corresponding to $\Delta V_{\rm max} = 0.05$ is not labelled.

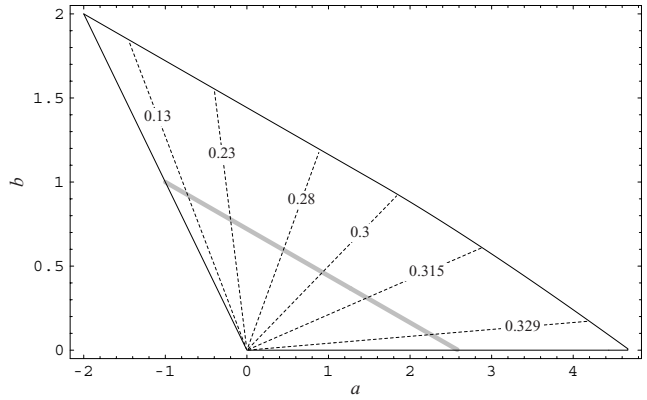

Figure 3. Ratio of the actual current density to the Goldreich–Julian current density $\iota(1)$ at the polar-cap boundary, where the minimum value of this ratio is achieved (see text). The dotted lines show contours of $\iota(1)$, labelled with the corresponding value of $\iota(1)$.

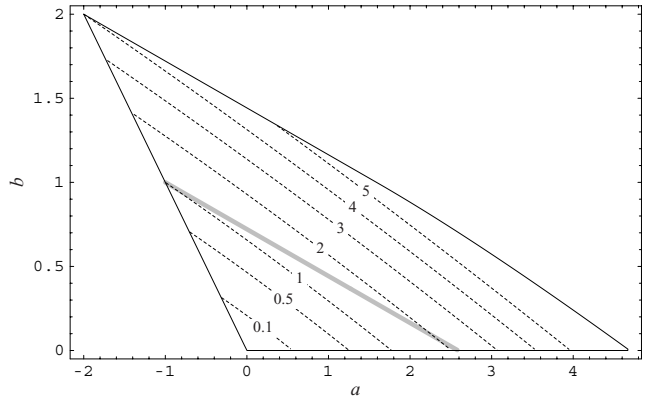

Figure 4. Spindown rate in terms of the Michel spindown rate. The dotted lines show contours of w, labelled with the corresponding value of w.

However, as we do not understand in detail the physics of non-stationary cascades, we cannot judge whether a particular form of $V(\psi)$ is admitted by the cascade physics or not. On the other hand, in young pulsars the average potential drop cannot be very large, because a small fraction of the vacuum potential drop would be sufficient for massive pair creation and screening of the accelerating electric field. At present, therefore, we can judge the reasonableness of a particular current density distribution only from the maximum value of the potential drop it requires. The electric potential given by equation (32) is known up to the additive constant V_0, which is the value of the accelerating potential at the polar-cap boundary. V_0 and thus the actual potential drop in the accelerating zone cannot be inferred from the physics of the magnetosphere, and is set by the physics of the polar-cap cascades. The only thing we can say about the maximum potential drop in the acceleration zone *along* field lines is that its absolute value is not smaller than the absolute value of the maximum potential drop of $V(\psi)$ *across* the polar cap.

Let us now consider possible values of the maximum potential drop across the polar cap of the pulsar. If the potential is a monotonic function of ψ in the polar cap, the maximum potential drop is the drop between the rotation axis and the polar-cap boundary. If the potential as a function of ψ has a minimum inside the polar cap, the maximum potential drop will be either between the axis and the minimum point, or between the edge and the minimum point. We analyse this issue in detail in Appendix B. In Fig. 2 the contour map of the maximum potential drop in the plane (a, b) is shown. The line given by equation (B1) is the line for which, for fixed a (or b), the smallest value of the potential drop across the polar cap is achieved. From this plot it is evident that, even if the potential drop in the polar cap is moderate, of the order of $\sim$10 per cent, there are force-free magnetosphere configurations for which the current density distribution deviates significantly from the Michel current density distribution. Thus even for young pulsars there may be some flexibility in the current density distribution admitted by the force-free electrodynamics.

Note that force-free magnetospheres impose different constraints on pulsars in aligned $\boldsymbol{\mu} \cdot \boldsymbol{\Omega} > 0$ and anti-aligned $\boldsymbol{\mu} \cdot \boldsymbol{\Omega} < 0$ configurations [pulsar and antipulsar in the terminology of Ruderman & Sutherland (1975)]. For pulsars, the accelerating potential is positive; that is, it increases from the surface of the NS towards the force-free zone above the pair-formation front. In the case of an antipulsar, the potential is negative: it decreases towards the pair-formation front, because positive charges are accelerated. Equations for the current density (15), (29) that we used to derive the equation for the electric potential (30) contain the expression for the GJ charge density as a factor, and, hence, the resulting expression for the electric potential is the same for each sign of the GJ current density. For pulsars, there is thus a *minimum* in the accelerating potential distribution; for antipulsars, the distribution of the accelerating electric potential has a *maximum*. Mathematically this results from different signs of the integration constant V_0.

4.3 Angular velocity

The normalized angular velocity of the open magnetic field lines in a force-free magnetosphere with the linear current density distribution (29) is given by

$$\beta(\psi) = \frac{2b + a\psi}{2 - \psi}. \tag{34}$$

For admitted current densities it grows with increasing ψ, because the first derivative $\mathrm{d}\beta/\mathrm{d}\psi$ for the admitted values of a, b is always non-negative. Thus the angular velocity either *increases* towards the polar-cap boundary or remains *constant* over the cap if $a = -b$. The latter case includes the Michel solution. The minimum value of β,

$$\beta_{\rm min} = b, \tag{35}$$

is achieved on the rotation axis, where $\psi = 0$, and the maximum value,

$$\beta_{\min} = 2b + a, \tag{36}$$

is achieved at the polar-cap boundary, where $\psi = 1$. Therefore, the open field lines can rotate more slowly, as well as faster than the NS, but the lines near the polar-cap boundary cannot rotate more slowly than the lines near the rotation axis.

4.4 Goldreich–Julian current density

An expression for the GJ current density in the polar cap can be obtained by substitution of the expression (34) for β into equation (20) for the GJ current density. We obtain

$$j_{\rm GJ}(\psi) = j^0_{\rm GJ}\,\frac{4b + a\psi(4-\psi)}{(\psi-2)^2}. \tag{37}$$

For the admitted values of the parameters a, b, the derivative $\mathrm{d}\, j_{\rm GJ}/\mathrm{d}\psi$ is always non-negative, and, hence, the GJ current density either *increases* towards the polar-cap boundary, or remains *constant* when $a = -b$. The actual current density, however, could decrease or increase towards the polar-cap edge.

For the charge-separated flow, the deviation of the current density from the GJ current density generates an accelerating or a decelerating electric field when $j < j_{\rm GJ}$ or $j > j_{\rm GJ}$, respectively. Although in non-stationary cascades the particle flow would not be charge-separated, the ratio of the actual current density to the GJ current density may give some clues on the cascade states required by a particular magnetosphere configuration. This ratio is given by

$$\iota(\psi) \equiv \frac{j(\psi)}{j_{\rm GJ}(\psi)} = \frac{(\psi-2)^2(b+a\psi)}{a\psi(4-\psi)+4b}. \tag{38}$$

For each admitted configuration, the current density is equal to the GJ current density on the rotation axis. For the admitted values of the parameters a, b the derivative $\mathrm{d}\iota/\mathrm{d}\psi$ is always negative, and, hence, the current density in terms of the GJ current density *decreases* towards the polar-cap boundary. Therefore, except on the rotation axis, the current density in the polar cap is always lower than the GJ current density. The relative deviation of the actual current density from the GJ current density is maximal at the polar-cap boundary:

$$\iota(1) = \frac{a+b}{3a+4b}. \tag{39}$$

Its maximum value, $\iota_{\max} = 1/3$, occurs when $b = 0$. Its minimum value, $\iota_{\min} = 0$, occurs when $a = -b$, which includes the case of the Michel current density distribution. The contours of $\iota(1)$ are shown in Fig. 3.

4.5 Spindown rate and the total energy of the electromagnetic field in the magnetosphere

In our notation, the spindown rate of an aligned rotator is (cf. equation 60 in Paper I)

$$W = W_{\rm md}\left|\int_0^{\Psi_{\rm pc}} S(\Psi)\beta(\Psi)\,\mathrm{d}\Psi\right|, \tag{40}$$

where $W_{\rm md}$ is the magnetodipolar energy losses defined as

$$W_{\rm md} = \frac{B_0^2 R_{\rm NS}^6 \Omega^4}{4c^3}. \tag{41}$$

Substituting the expression for the poloidal current (12) and using the normalized flux function ψ we obtain

$$W = W_{\rm md}\,\Psi_{\rm pc}^2 \int_0^1 \beta^2(\psi)\psi(2-\psi)\,\mathrm{d}\psi. \tag{42}$$

The expression for the spindown rate in the Michel solution,

$$W_{\rm M} = \frac{2}{3}\Psi_{\rm pc}^2 W_{\rm md}, \tag{43}$$

differs from the spindown rate obtained in the numerical simulations of the corotating aligned rotator magnetosphere by a constant factor. It has, however, a very similar dependence on the size of the corotating zone x_0 (cf. equations 62 and 63 in Paper I). As our solutions are obtained in the split-monopole approximation, they should differ from the real solution in approximately the same way as the Michel solution does. Because of this, it would be more appropriate to normalize the spindown rate to the spindown rate in the Michel split-monopole solution. By doing this we will be able to study the effect of differential rotation on the energy losses separately from the dependence of the spindown rate on the size of the corotating zone.

For the normalized spindown rate in the considered case of a linear current density we obtain

$$w \equiv \frac{W}{W_{\rm M}} = 4a^2(3\log 2 - 2) + 3ab(8\log 2 - 5) + 6b^2(2\log 2 - 1). \tag{44}$$

In Fig. 4 the contour lines of w are shown in the domain of admitted values for the parameters a, b. We see that the spindown rate can vary significantly, from zero to a value exceeding the Michel energy losses by a factor of $\approx$6. It increases with increasing values of the parameters a, b, and decreases with decreasing values. This dependence of the spindown rate on the parameters a, b is caused by an increase or decrease of the total poloidal current in the magnetosphere, respectively.

The total energy of the magnetosphere can be estimated from the split-monopole solution. Using the formula (C7) derived in Appendix C we have for the total energy of the electromagnetic field

$$\mathcal{W} \simeq \mathcal{W}_{\rm pol} + \frac{R - R_{\rm NS}}{c} W, \tag{45}$$

where $\mathcal{W}_{\rm pol}$ is the total energy of the poloidal magnetic field and R is the radius of the magnetosphere. The first term in our approximation is the same for all magnetosphere configurations; the difference in the total energy arises from the second term. Hence, the contours of constant total energy in the plane (a, b) have the same form as the contours of the spindown rate W shown in Fig. 4. The total energy of the magnetosphere increases with increasing values of the parameters a, b; that is, it increases with increasing poloidal current.

4.6 Example solutions

As examples we consider here the properties of two particular solutions in detail. We chose these solution because either their current density or their potential drop seems to correspond to 'natural' states of the polar-cap cascades. Although we do not claim that either of the solutions can be realized as a real pulsar configuration, knowledge of their properties may be helpful in understanding the physical conditions that the polar-cap cascades should adjust to.

4.6.1 Configurations with constant current density

We first consider the case in which the current density is constant[5] over the polar cap; that is, $a = 0$ and $j = b j^0_{\rm GJ}$. A constant-density distribution will be produced by cascades in their 'natural' state if

[5]For this class of solutions we label all physical quantities with the superscript 'c'.

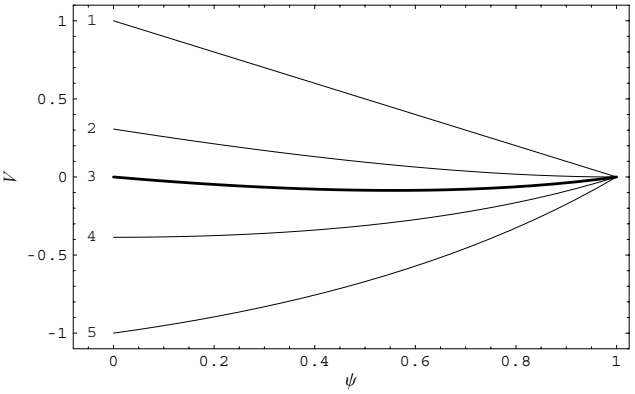

Figure 5. Electric potential in the polar cap of the pulsar as a function of the normalized flux function ψ for magnetosphere configurations with a constant current density across the cap. In all cases V_0 is set to zero. Numbers near the lines correspond to the following values of b. 1: $b = 0$; 2: $b = 0.5$; 3: $b = b_{\max}/2$; 4: $b = 1$; 5: $b = b_{\max}$. The line corresponding to the minimum potential drop across the cap is shown by the thick solid line (line 3).

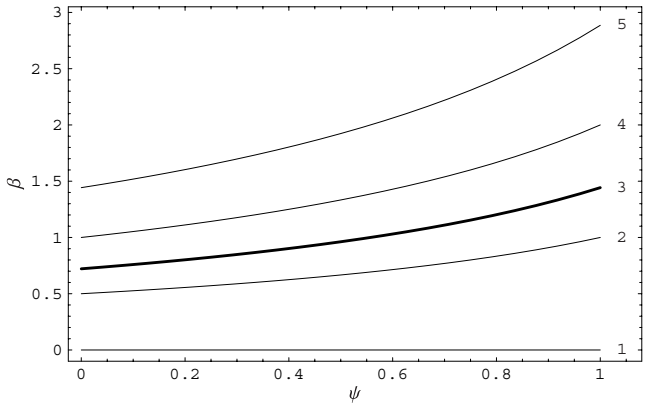

Figure 6. Normalized angular velocity of the open magnetic field lines as a function of the normalized flux function ψ for magnetosphere configurations with a constant current density across the cap. Labelling of the curves is as in Fig. 5.

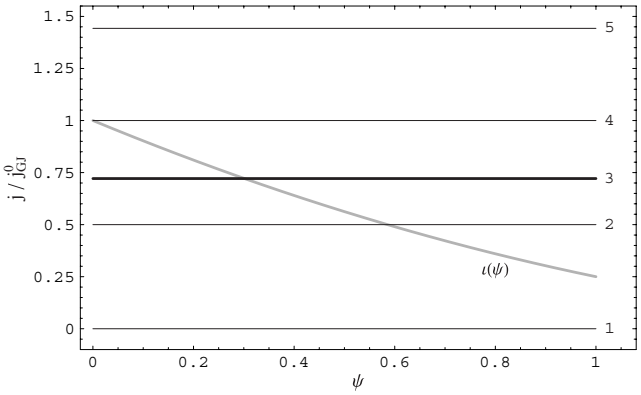

Figure 7. Current density as a function of the normalized flux function ψ for magnetosphere configurations with a constant current density across the cap. Labelling of the curves is as in Fig. 5. The thick grey line shows the ratio of the actual current density to the GJ current density $\iota(\psi)$. For this case $\iota(\psi)$ is the same for all solutions.

the current adjustment proceeds locally, without a strong influence from the current along adjacent field lines. The electric potential in that case is

$$V^{\rm c}(\psi) = V_0 + 1 - \psi - 2b\log(2-\psi). \tag{46}$$

This potential has the following properties (see Fig. 5, where $V(\psi)$ is shown for several values of b, assuming for the sake of simplicity that $V_0 = 0$):

(i) the admitted values of the current density in the polar cap of the pulsar are within the interval $[0, b_{\max}]$, where $b_{\max} = 1/\log 2 \simeq 1.443$.

(ii) if $0 \leqslant b < b_{\max}/2 \simeq 0.721$, the value of the electric potential at the rotation axis $V^{\rm c}$ (0) is larger than the value at the polar-cap edge, $V^{\rm c}$ (1), i.e. $V^{\rm c}$ (0) > $V^{\rm c}$ (1)

(iii) if $b_{\max}/2 < b \leqslant b_{\max}$, the value of the electric potential at the rotation axis $V^{\rm c}$ (0) is smaller than the value at the polar-cap edge, $V^{\rm c}$ (1), i.e. $V^{\rm c}$ (0) < $V^{\rm c}$ (1).

(iv) if $0 \leqslant b \leqslant 1/2$ or $1 \leqslant b \leqslant b_{\max}$, the potential is a monotonic function of ψ; if $1/2 < b < b_{\max}$, it has a minimum.

(v) At the point $b = b_{\max}/2$, the maximum potential drop across the polar cap reaches its minimum value, $\Delta V_{\max} = 0.086$.

The reason for this behaviour of the potential is easy to understand from Fig. B1 in Appendix B. The critical points at which $V(\psi)$ changes its behaviour are the points at which the line $a = 0$ intersects the boundaries of the regions I, II, III, and IV.

The angular velocity of the open magnetic field lines is

$$\beta^{\rm c}(\psi) = \frac{2b}{2-\psi}. \tag{47}$$

The distribution of the corresponding angular velocity is shown in Fig. 6. For $b > 1$ the angular velocity of rotation of all open magnetic field lines is greater than the angular velocity of the NS. For $b < 1/2$ all magnetic field lines rotate more slowly than the NS. For $1/2 < b < 1$ some open field lines near the rotation axis rotate more slowly than the NS, whereas other open field lines rotate faster than the NS.

The current density distribution in terms of the GJ current density is

$$\iota^{\rm c}(\psi) = \frac{1}{4}(2-\psi)^2, \tag{48}$$

which does not depend on the value of the parameter b. The current density is always sub-Goldreich–Julian, except on the rotation axis, where it is equal to the GJ current density (see Fig. 7).

The normalized spindown rate for the considered case has a simple quadratic dependence on the current density:

$$w^{\rm c} = 6(\log 4 - 1)b^2. \tag{49}$$

This dependence is shown in Fig. 8. The energy losses in a configuration with a constant current density cannot be higher than ≈4.82 of the energy losses in the corresponding Michel solution.

It is worthwhile to mention the case $b = 1$ separately, as it is 'the most natural' state for the space charge-limited particle flow, for which the current density at the surface of the NS is equal to the corotational GJ current density. In Figs 5, 6 and 7 the lines corresponding to this case are labelled with a '3'. The maximum potential drop for the configuration with the current density distribution equal to the corotational GJ current density is $\Delta V_{\max} = 0.386$, and the angular velocity of the open field lines varies from 1 at the rotation axis to 2 at the polar-cap boundary.

4.6.2 Configurations with the smallest potential drops

For the next example we consider the case in which the maximum potential drop across the polar cap for a fixed value of either a or b is

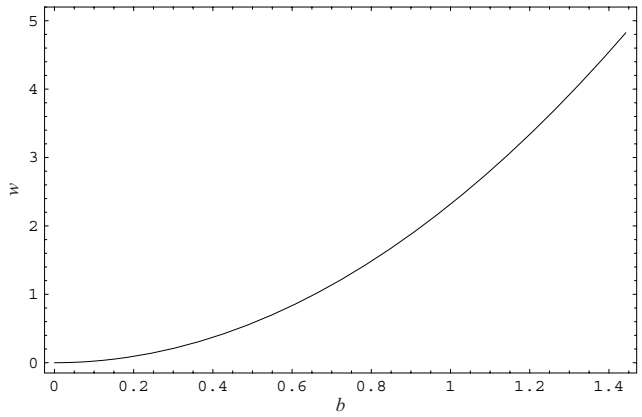

Figure 8. Spindown rate of an aligned rotator normalized to the spindown rate in the Michel solution for magnetosphere configurations with a constant current density across the cap as a function of the current density in the polar cap (parameter b).

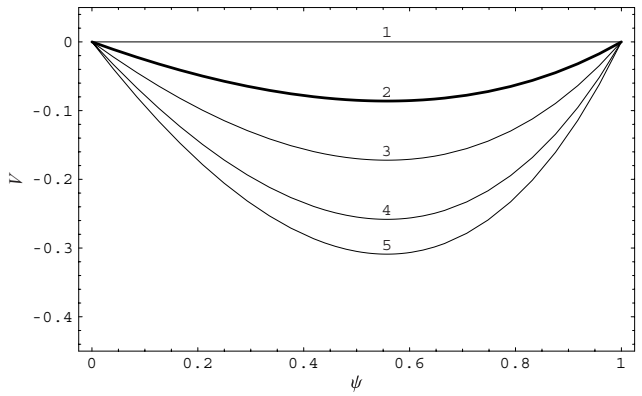

Figure 9. Electric potential in the polar cap of the pulsar as a function of the normalized flux function ψ for magnetosphere configurations with the smallest potential drop across the cap. In all cases V_0 is set to zero. Numbered lines correspond to the following values of a. 1: $a = -1$ (Michel's solution); 2: $a = 0$ (solution with a constant current density); 3: $a = 1$; 4: $a = 2$; 5: $a = 1/(\log 4 - 1)$.

minimal[6]. The points corresponding to such values of the parameters are shown as a thick grey line in Figs 2, 3 and 4. The equation for this line in the plane (a, b) is derived in Appendix B, equation (B1). In some sense this is an optimal configuration for the cascade zone, because for a fixed value of the current density at a given magnetic field line such a configuration requires the smallest potential drop for the admitted configurations. The accelerating potential for the considered class of configurations is

$$V^{\rm s}(\psi) = V_0 - (a+1)\left[\psi + \frac{\log(1-\psi/2)}{\log 2}\right]. \tag{50}$$

The potential is shown as a function of ψ in Fig. 9 for several cases, assuming for the sake of simplicity a zero potential drop at the polar-cap boundary. The potential always has a minimum at the point

$$\psi^{\rm s}_{\rm min} = 2 - \frac{1}{\log 2} \simeq 0.557; \tag{51}$$

[6]For this class of solutions we label all physical quantities with the superscript 's' (smallest).

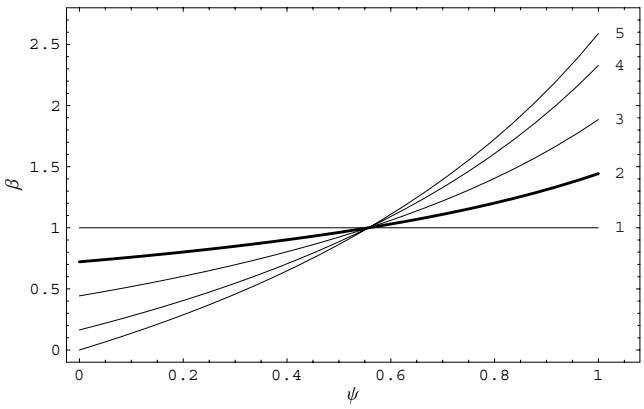

Figure 10. Normalized angular velocity of the open magnetic field lines as a function of the normalized flux function ψ for magnetosphere configurations with the smallest potential drop across the cap. Labelling of the curves is as in Fig. 9.

the position of this minimum does not depend of the values of a, b. The minimum value of the maximal potential drop across the cap, $\min(\Delta V_{\rm max}) = 0$, is achieved at the left end of the grey line, at the point $(a = -1,\ b = 1)$ corresponding to the Michel solution. The maximum potential drop across the gap for this class of configurations, $\max(\Delta V_{\rm max}) = 0.309$, is achieved at the right end of the grey line, at the point $(a = 1/(\log 4 - 1),\ b = 0)$.

The angular velocity of the open field lines is

$$\beta^{\rm s}(\psi) = \frac{a+1}{(2-\psi)\log 2} - a. \tag{52}$$

The distribution of $\beta^{\rm s}(\psi)$ is shown in Fig. 10. For values of ψ lower than $\psi^{\rm s}_{\rm min}$, where the minimum value of the potential is achieved, β is not greater than 1; for larger values, β is not less than 1. As the maximum potential drop increases, the variation of the angular velocity across the polar cap becomes larger.

The current density distribution in the considered case has the form

$$j^{\rm s}(\psi) = a\psi + \frac{a(1-\log 4)+1}{\log 4}. \tag{53}$$

This distributions is shown in Fig. 11. All curves pass through the point $\hat{\psi} = 1 - 1/\log 4$, where the current density is $j^{\rm s}(\hat{\psi}) = j^0_{\rm GJ}/\log 4$.

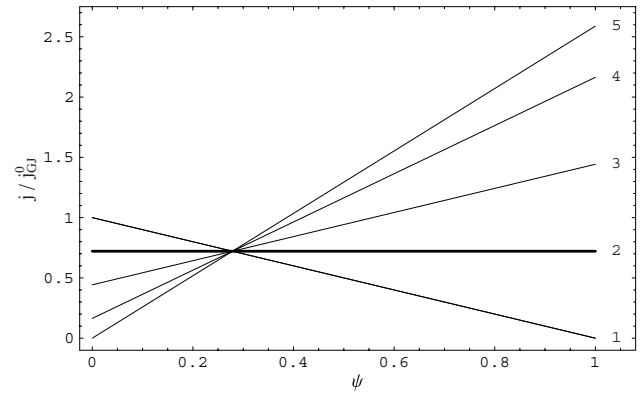

Figure 11. Current density as a function of the normalized flux function ψ for magnetosphere configurations with the smallest potential drop across the cap. Labelling of the curves is as in Fig. 9.

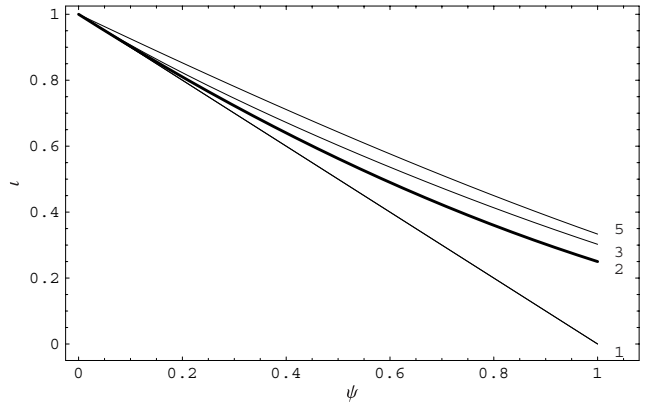

Figure 12. Ratio of the actual current density to the GJ current density ι as a function of the normalized flux function ψ for magnetosphere configurations with the smallest potential drop across the cap. Labelling of the curves is as in Fig. 9.

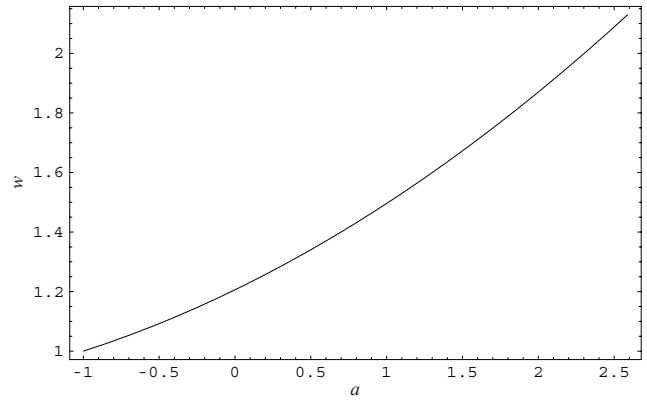

Figure 13. Spindown rate of an aligned rotator normalized to the spindown rate in the Michel solution for magnetosphere configurations with the smallest potential drop across the cap as a function of the parameter a.

The current density distribution in terms of the Goldreich–Julian current density is

$$\iota^{\rm s}(\psi) = \frac{(\psi-2)^2[(\psi-1)a\log 4 + a + 1]}{\psi(4-\psi)a\log 4 + 4a(1-\log 4) + 4}. \tag{54}$$

It decreases monotonically from 1 at the rotation axis to its minimum value at the polar-cap boundary (see Fig. 12). This minimum value is in the range [0, 1/3]; the lower value corresponds to the left end of the grey curve (the Michel solution), and the upper value corresponds to the right end of the grey line. The outflow is sub-GJ everywhere except on the rotation axis.

The normalized spindown rate for the considered case is

$$w^{\rm s} = \frac{1}{2\log^2 2}\{[2\log^2 2 - 3(1-\log 2)]a^2 - 3(2-3\log 2)a - 3(1-2\log 2)\}. \tag{55}$$

It is shown as a function of the parameter a in Fig. 13. It can be seen that for the considered configuration the spindown rate as a function of the parameter a increases more slowly than the spindown rate for configurations with a constant current density as a function of b (cf. Fig. 8). The energy losses cannot be higher than $\approx$2.13 of the energy losses in the corresponding Michel solution.

5 DISCUSSION

The main aim of this paper was to study the range of admitted current density distributions in the force-free magnetosphere of an aligned rotator. Taking into account that this subject has not previously been studied in detail, the linear model used in this work is, in our opinion, an adequate approach to the problem. Knowledge of the behaviour of the magnetosphere in response to various potential drops in the polar cap is likely to be very useful for future modelling of non-stationary polar-cap cascades. This formalism could be used as a tool for allowing a quick judgement to be made on whether a particular model of the polar-cap cascades is compatible with a force-free magnetosphere or not. It may also provide a clue as to how the magnetosphere would respond to a particular current density distribution obtained at some step in the course of the numerical solution. Although the analytical model presented here needs to be refined in numerical simulations, the presence of some analytical relationships should be very useful in the numerical modelling of cascades.

We have considered here a simple case in which the current density in the polar cap of a pulsar is a linear function of the magnetic flux. However, the generalization of the model to a more complicated shape of the current density distribution is straightforward. One should proceed with the steps described at the beginning of Section 3 for the desired form of the current density distribution. The resulting equation for the electric potential will be an ordinary differential equation, and the numerical solution of such an equation for any given current density will not be a problem.

The conclusion we wish to emphasize from the presented results is that, even for a fairly moderate potential drop in the acceleration zone, the current density distribution can deviate significantly from the 'canonical' Michel distribution. We note that even for dipole geometry the current density distribution is similar to the Michel distribution if all magnetic field lines corotate with the NS (see Paper I). In particular, a magnetosphere configuration with a constant current density at the level of 73 per cent of the GJ current density at the NS surface would require a potential drop in the acceleration zone of the order of 10 per cent of the vacuum potential drop. For time-dependent cascades this may be realized even for young pulsars. It should be noted, however, that for young pulsars a potential drop of the order of 10 per cent of the vacuum drop could cause overheating of the polar cap by means of the particles accelerated towards the NS (e.g. Harding & Muslimov 2001; Harding & Muslimov 2002). In that sense, such a potential drop may be too large for young pulsars. On the other hand, without knowledge of the dynamics of non-stationary cascades it is in our opinion too soon to exclude the possibility of such configurations for young pulsars, as in a non-stationary regime the heating of the cap may not be as strong as in stationary cascades (see Levinson et al. 2005).

We used a split-monopole approximation for the poloidal current density distribution in the magnetosphere, which produces accurate results only for configurations with a very small corotating zone, when the size of the zone is much less than the size of the light cylinder $x_0 \ll 1/\beta(\Psi_{\rm pc})$ (see Fig. 1). For the (most interesting) case for which these sizes are comparable, the results obtained in this work can be considered only as a zero approximation to the real problem. We note here an important modification introduced by the dipole geometry of the magnetic field. For the dipole geometry there will be some magnetic field lines that bend to the equatorial plane at the light cylinder. For these field lines the second term on the right-hand side of equation (4) [which in cylindrical coordinates

(ϖ, ϕ, z) is $2\beta\partial_{\varpi}\Psi$] will be negative, and in order to obtain a positive current density along these lines a steeper dependence of β on ψ is necessary. As a result, the potential drop in the dipole geometry will be higher than that obtained in our approximation. Figuratively speaking, in our model we could correct only for the decrease of the electric current density towards the polar-cap boundary present in the Michel solution, but not for the negative current density near the edge of the polar cap that is present in the dipole geometry for configurations with $\boldsymbol{x}_0 > 0.6$. On the other hand, if $\beta(\Psi_{\rm pc}) > 1$, the size of the corotating zone can be smaller as well as greater[7] than the light-cylinder radius at the last open field line. In the latter case there should be fewer magnetic field lines that bend towards the equatorial plane than in the first case, cf. Fig. 1 cases I and II. Hence, the correction introduced by the dipolar field geometry for some subset of our solutions will be non-monotonic as the size of the corotating zone x_0 increases. There is therefore still a possibility that a moderate potential drop could allow a large variety of current densities, although this issue needs careful investigation.

In this paper we have ignored the electrodynamics of the polar-cap zone. Although without a theory of time-dependent cascades we cannot put more limitations on the electric potential than the limitation we used in Section 2.2, there is an additional limitation arising from the basic electrodynamics, namely that the accelerating potential near a conducting wall, which the current sheet at the polar-cap edge is believed to be, should approach zero. We could, however, speculate that there is a thin non-force-free zone at the edge of the polar cap where the adjustment of the potential occurs. In other words, the return current may flow only in a part of the non-force-free zone. Because of this, that limitation would not place strong restrictions on our solution.

Finally, we would like to discuss briefly the issue of the pulsar braking index. If the inner pulsar magnetosphere is force-free, the spindown rate of an aligned pulsar as a function of the angular velocity will deviate from the power law $W \propto \Omega^4$ if the size of the corotating zone and/or the distribution $\beta(\psi)$ change with time. The assumption that these 'parameters' are time-dependent seems to us to be natural, because with the ageing of the pulsar the conditions in the polar-cap cascade zone change and the magnetosphere should adjust to these new conditions. In the framework of our model we could make some simple estimations of how the braking index of the pulsar is affected by the changes of these two 'parameters'.

As an example we consider the case for which the pulsar magnetosphere evolves through a set of configurations with a constant current density. The spindown rate for such configurations is

$$W \propto \Omega^4 \Psi_{\rm pc}^2 b^2 \sim \Omega^4 x_0^{-2} b^2, \tag{56}$$

where we estimate $\Psi_{\rm pc}$ assuming a dipole field in the corotation zone. If b and/or x_0 are functions of time, the spindown rate will be different from the spindown of a dipole in a vacuum. If at some moment the dependence of the size of the corotating zone and the current density on Ω could be approximated as $x_0 \propto \Omega^{\xi}$ and $b \propto \Omega^{\zeta}$, respectively, the braking index of the pulsar measured at that time would be

$$n = 3 - 2\xi + 2\zeta. \tag{57}$$

It can be seen that the deviation of the braking index from the 'canonical' value, being equal to 3, would be by a factor of two larger than the dependence of b and x_0 on Ω. The braking index could be smaller as well as larger than 3, depending on the sign of the expression $\zeta - \xi$. For instance, if in an old pulsar the potential drop increases and, as a consequence, the current density decreases, ζ is positive, and the braking index could be *greater* than 3. We note that there is evidence for such values of the braking index for old pulsars (Arzoumanian, Chernoff & Cordes 2002). On the other hand, if x_0 decreases with time, as was proposed in Paper I for young pulsars, the braking index would be less than 3. However, even for an aligned rotator a more complicated dependence of the braking index on the pulsar age may be possible. In reality, the evolution of the pulsar magnetosphere will be more complicated, and a steeper as well as a more gradual dependence of the braking index on the current density will be possible. This will result in a wide range of possible values of the pulsar braking index.

[7]For the closed magnetic field lines the angular velocity is Ω, and they are still inside *their* light cylinder; the adjustment of the angular velocity occurs in the current sheet, which is a non-force-free domain.

ACKNOWLEDGMENTS

I acknowledge J. Arons, J. Gil, Yu. Lyubarsky and G. Melikidze for fruitful discussions. I would like to thank J. Arons for useful suggestions on a draft version of the article. This work was partially supported by the Russian grants N.Sh.-5218.2006.2, RNP.2.1.1.5940, N.Sh.-10181.2006.2 and by the Israel–US Binational Science Foundation and an Israeli Science Foundation Center of Excellence Grant.

REFERENCES

Al'Ber Y. I., Krotova Z. N., Eidman V. Y., 1975, Astrofizika, 11, 189
Arons J., 1979, Space Sci. Rev., 24, 437
Arzoumanian Z., Chernoff D. F., Cordes J. M., 2002, ApJ, 568, 289
Beskin V. S., 2005, Osesimmetrichnye Stacionarnye Techeniya v Astrofizike. (Axisymmetric Stationary Flows in Astrophysics) Fizmatlit, Moscow (in Russian)
Beskin V., Gurevich A., Istomin Y., 1993, Physics of the Pulsar Magnetosphere. Cambridge Univ. Press, Cambridge
Blandford R. D., Znajek R. L., 1977, MNRAS, 179, 433
Bucciantini N., Thompson T. A., Arons J., Quataert E., Del Zanna L., 2006, MNRAS, 368, 1717
Contopoulos I., 2005, A&A, 442, 579
Contopoulos I., Kazanas D., Fendt C., 1999, ApJ, 511, 351
Fawley W. M., 1978, PhD thesis, Univ. California, Berkeley
Goldreich P., Julian W. H., 1969, ApJ, 157, 869
Goodwin S. P., Mestel J., Mestel L., Wright G. A. E., 2004, MNRAS, 349, 213
Gruzinov A., 2005, Phys. Rev. Lett., 94, 021101
Harding A. K., Muslimov A. G., 2001, ApJ, 556, 987
Harding A. K., Muslimov A. G., 2002, ApJ, 568, 862
Komissarov S. S., 2006, MNRAS, 367, 19
Levinson A., Melrose D., Judge A., Luo Q., 2005, ApJ, 631, 456
Lyubarskij Y. E., 1992, A&A, 261, 544
McKinney J. C., 2006, MNRAS, 368, L30
Michel F. C., 1973a, ApJ, 180, 207
Michel F. C., 1973b, ApJ, 180, L133
Michel F. C., 1991, Theory of Neutron Star Magnetospheres. University of Chicago Press, Chicago, IL
Okamoto I., 1974, MNRAS, 167, 457
Ruderman M. A., Sutherland P. G., 1975, ApJ, 196, 51
Scharlemann E. T., Wagoner R. V., 1973, ApJ, 182, 951
Scharlemann E. T., Arons J., Fawley W. M., 1978, ApJ, 222, 297
Spitkovsky A., 2006, ApJ, 648, L51
Timokhin A. N., 2006, MNRAS, 368, 1055
Timokhin A. N., 2007, Ap&SS, 308, 575

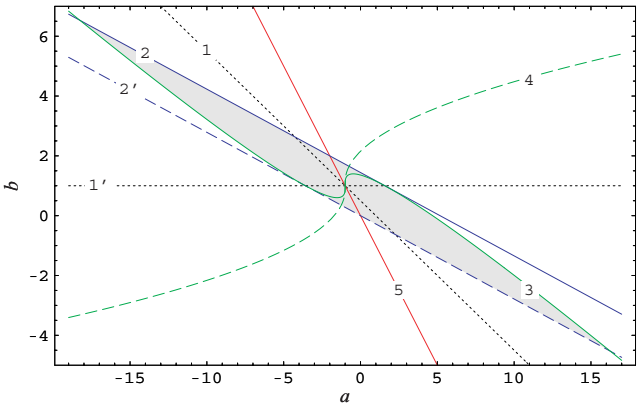

Figure A1. Values of the parameters a and b admitted by the requirement that the maximum potential drop across the polar cap is less than the vacuum potential drop. The dotted lines 1 and 1′ show the boundary of the region where the potential has an extremum in the polar cap. Line 2 corresponds to $\Delta V_{10} = 1$, and line 2′ corresponds to $\Delta V_{10} = -1$. Line 3 corresponds to $|\Delta V_{1e}| = 1$, and line 4 corresponds to $|\Delta V_{0e}| = 1$. Line 2′ corresponds to $b = -a$. The resulting admitted region is shown in grey. See text for further explanations.

APPENDIX A: ADMITTED CURRENT DENSITY

The second derivative of $V(\psi)$ with respect to ψ is

$$V''(\psi) = 2\,\frac{a+b}{(2-\psi)^2}. \tag{A1}$$

For fixed a and b, the second derivative never changes sign, and hence $V(\psi)$ has a single extremum. If $a + b > 0$, $V(\psi)$ has a single minimum; in the plane (a, b) shown in Fig. A1 these points lie to the right of line 5. If $a + b < 0$, $V(\psi)$ has a single maximum, and such points lie to the left of line 5 in Fig. A1. The potential reaches its extremum value at the point

$$\psi_{\rm ex} = 2\,\frac{1-b}{a+1}. \tag{A2}$$

This point lies in the interval [0, 1] if

$$\begin{aligned} 1 \geqslant b \geqslant \frac{1-a}{2}, &\quad \text{for } a > -1; \\ 1 \leqslant b \leqslant \frac{1-a}{2}, &\quad \text{for } a < -1. \end{aligned} \tag{A3}$$

In Fig. A1, points at which these conditions are satisfied lie between the lines 1 and 1′, in the region where the angle between the lines is acute. Line 1 corresponds to values of a, b for which the extremum of the potential is reached at the polar-cap boundary. Line 1′ corresponds to values of a, b for which the extremum of the potential is reached at the rotation axis.

If $\psi_{\rm ex}$ is outside the interval [0, 1], $V(\psi)$ is a monotonic function of ψ in the polar cap of the pulsar, and the maximum potential drop is the potential drop between the edge of the polar cap and the rotation axis. In this case, condition (9) takes the form

$$|\Delta V_{10}| \leqslant 1, \tag{A4}$$

where $\Delta V_{10} \equiv V(1) - V(0)$ is the potential drop between the boundary of the polar cap and the rotation axis. In terms of the parameters a, b it can be written as

$$a\,\frac{1-\log 4}{\log 4} \leqslant b \leqslant \frac{1}{\log 2} + a\,\frac{1-\log 4}{\log 4}. \tag{A5}$$

In Fig. A1 points satisfying this condition lie between lines 2 and 2′. In the region where the angle between lines 1 and 1′ is obtuse (here the point $\psi_{\rm ex}$ is outside the interval [0, 1]), the lines 2 and 2′ set the boundaries for admitted values of the parameters a and b.

If the electric potential reaches its extremum value inside the polar cap, the maximum potential drop is achieved either between the extremum point and the edge of the polar cap, or between the extremum point and the rotation axis. In this case, condition (9) takes the form

$$\max(|\Delta V_{0e}|, |\Delta V_{1e}|) \leqslant 1, \tag{A6}$$

where $\Delta V_{0e} \equiv V(0) - V(\psi_{\rm ex})$ is the potential drop between the rotation axis and the point $\psi_{\rm ex}$, and $\Delta V_{1e} \equiv V(1) - V(\psi_{\rm ex})$ is the potential drop between the polar-cap boundary and the point $\psi_{\rm ex}$. The expression for the extremum value of V is non-linear with respect to a, b:

$$V(\psi_{\rm ex}) = V_0 - 1 + a + 2b - 2(a+b)\log\left[\frac{2(a+b)}{1+a}\right], \tag{A7}$$

and condition (A6) in terms of a, b should be evaluated numerically. For a fixed a, the derivatives of ΔV_{0e} and ΔV_{1e} with respect to b are

$$\frac{{\rm d}\,\Delta V_{0e}}{{\rm d}\,b} = 2\log\left(\frac{a+b}{1+a}\right), \tag{A8}$$

$$\frac{{\rm d}\,\Delta V_{1e}}{{\rm d}\,b} = 2\log\left(\frac{a+b}{1+a}\right) + \log 4. \tag{A9}$$

If $\psi_{\rm ex} \in [0, 1]$, condition (A3) is fulfilled, ${\rm d}\,\Delta V_{1e}/{\rm d}\,b$ is positive and ${\rm d}\,\Delta V_{0e}/{\rm d}\,b$ is negative. So, for a fixed a when $\psi_{\rm ex} \in [0, 1]$, ΔV_{0e} decreases and ΔV_{1e} increases with increasing b.

In Fig. A1, line 3 represents points for which $|\Delta V_{1e}| = 1$, and line 4 represents points for which $|\Delta V_{0e}| = 1$. To the right of line 5, $V(\psi)$ has a minimum, and the lines 3 and 4 represent points for which $\Delta V_{1e} = 1$ and $\Delta V_{0e} = 1$, respectively. To the left of line 5, $V(\psi)$ has a maximum, and here the lines 3 and 4 correspond to $\Delta V_{1e} = -1$ and $\Delta V_{0e} = -1$. Line 4 always lies outside the region between lines 1 and 1′, and, hence, the absolute value of the potential drop between the extremum point and the rotation axis $|\Delta V_{0e}|$ never achieves the vacuum potential drop when the extremum point is inside the interval (0, 1).

ΔV_{1e} increases with increasing b. So, below curve 3 to the right of line 5, and above curve 3 to the left of line 5, $|\Delta V_{1e}|$ is less than 1. Hence, when $\psi_{\rm ex} \in [0, 1]$ (a, b are in the region between lines 1 and 1′), the admitted values of a and b are limited by the lines 3 and 2′ to the left of line 5, and by lines 2 and 3 to the right of line 5.

Combining all the discussed restrictions we obtain the region of admitted values of the parameters a and b, shown as the grey area in Fig. A1 .

APPENDIX B: THE MAXIMUM POTENTIAL DROP ACROSS THE POLAR CAP

In Fig. B1 the dotted lines 1 and 1′ limit the region[8] in the parameter space (a, b) where the potential in the polar cap is a non-monotonic function of ψ, and it has a minimum at some point $\psi_{\rm ex} \in (0, 1)$ (see Appendix A). In the regions III and IV the potential $V(\psi)$ is a monotonic function of ψ.

[8]Regions I and II together.

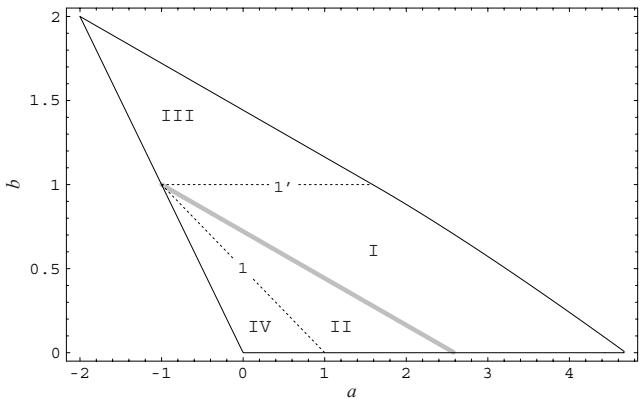

Figure B1. Region of admitted values of the parameters a and b corresponding to current densities of the same sign as the Goldreich–Julian current density. The dotted line 1 shows points for which $\Delta V_{1e} = 0$; line $1'$, points for which $\Delta V_{0e} = 0$. The thick grey line shows points for which $|\Delta V_{0e}| = |\Delta V_{1e}|$. In region I, $\Delta V_{max} = \Delta V_{1e}$; in region II, $\Delta V_{max} = \Delta V_{0e}$; and in regions II and IV, $\Delta V_{max} = |\Delta V_{10}|$. See text for further explanations.

The potential drop $\Delta V_{0e} \equiv V(0) - V(\psi_{ex})$ between the rotation axis and the point ψ_{ex} where $V(\psi)$ achieves its minimum value for a fixed a decreases with increasing b. For a, b on line $1'$, ψ_{ex} is on the rotation axis, and $\Delta V_{0e} = 0$ there. The potential drop $\Delta V_{1e} \equiv V(1) - V(\psi_{ex})$ between the polar-cap boundary and the point ψ_{ex} for a fixed a increases with increasing b. For a, b on line 1, ψ_{ex} is at the polar-cap boundary and $\Delta V_{1e} = 0$. Therefore, ΔV_{0e} increases in the direction from line $1'$ to line 1, and ΔV_{1e} increases in the direction from line 1 to line $1'$.

Along some line between lines $1'$ and 1 the potential drops ΔV_{0e} and ΔV_{1e} become equal. This means that the potential drop $\Delta V_{10} \equiv V(1) - V(0)$ between the polar-cap edge and the rotation axis is zero there. The equation for this line is easily obtained from the requirement $\Delta V_{10} = 0$:

$$b = \frac{1}{\log 4} + a\frac{1 - \log 4}{\log 4}. \tag{B1}$$

This line is shown in Fig. B1 as the thick grey line. Above the grey line $\Delta V_{1e} > \Delta V_{0e}$, and below it $\Delta V_{1e} < \Delta V_{0e}$. Hence, the line given by equation (B1) is the line for which the maximum potential drop across the polar cap achieves its minimum value for fixed a or b.

Taking all this into account we conclude that the maximum potential drop across the polar cap ΔV_{max} is equal to the following potential drops: in region I, to ΔV_{1e}; in region II, to ΔV_{0e}; and in regions III and IV, to $|\Delta V_{0e}|$.

APPENDIX C: ENERGY OF THE ELECTROMAGNETIC FIELD IN THE SPLIT-MONOPOLE CONFIGURATION

The energy density of the electromagnetic field in the magnetosphere is

$$w = \frac{1}{8\pi}\left(E^2 + B_{pol}^2 + B_\phi^2\right). \tag{C1}$$

For the split-monopole solution, when $\Psi = \Psi_{pc}(1 - \cos\theta)$, the non-zero components of the electric and magnetic fields are

$$E_\theta = -\frac{\mu}{R_{LC}^3}\Psi_{pc}\beta\frac{\sin\theta}{r}, \tag{C2}$$

$$B_r = \frac{\mu}{R_{LC}^3}\frac{\Psi_{pc}}{r^2}, \tag{C3}$$

$$B_\phi = -\frac{\mu}{R_{LC}^3}\Psi_{pc}\beta\frac{\sin\theta}{r}. \tag{C4}$$

The electric field is therefore equal to the toroidal magnetic field: $E_\theta = B_\phi$. The total energy of the magnetosphere is then

$$\mathcal{W} = \frac{1}{8\pi}\int\left(B_r^2 + 2E_\theta^2\right)\,\mathrm{d}V. \tag{C5}$$

On the other hand, the energy losses are

$$W = \int_{4\pi} c\,\frac{[\boldsymbol{E}\times\boldsymbol{B}]_r}{4\pi}\,\mathrm{d}\tilde{\Omega} = \int_{4\pi} c\,\frac{E_\theta^2}{4\pi}\,\mathrm{d}\tilde{\Omega}, \tag{C6}$$

where $\tilde{\Omega}$ is a solid angle. Using equations (C6) and (C3) we can rewrite expression (C5) for the total energy of the electromagnetic field as

$$\mathcal{W} = \frac{W_{md}}{c}\,\frac{\Psi_{pc}^2 R_{LC}^2}{2}\left(\frac{1}{R_{NS}} - \frac{1}{R}\right) + \frac{W}{c}(R - R_{NS}), \tag{C7}$$

where R is the size of the magnetosphere, i.e. the distance up to which its dynamics is determined by the central object. W_{md} represents the magnetodipolar energy losses, given by equation (41). The first term represents the total energy of the poloidal magnetic field and is the same for all configurations with different potential drops. The second term, being the sum of the energies of the electric field and the toroidal component of the magnetic field, is different for different values of the accelerating potential. It is directly proportional to the energy losses in a particular configuration.

This paper has been typeset from a TEX/LATEX file prepared by the author.